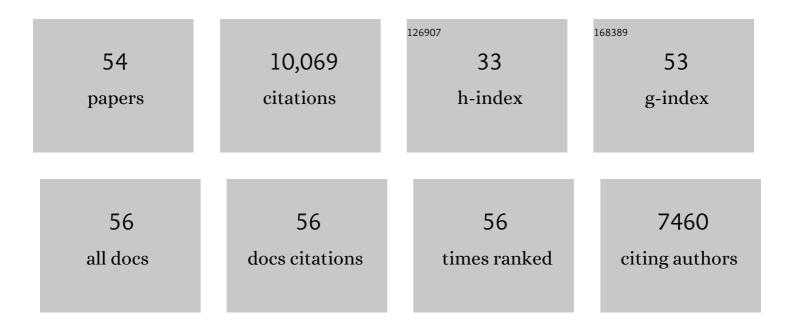
Omar Torres

List of Publications by Year in descending order

Source: https://exaly.com/author-pdf/7620484/publications.pdf Version: 2024-02-01



#	Article	IF	CITATIONS
1	Environmental characterization of global sources of atmospheric soil dust identified with the NIMBUS 7 Total Ozone Mapping Spectrometer (TOMS) absorbing aerosol product. Reviews of Geophysics, 2002, 40, 2-1.	23.0	2,380
2	Tropospheric Aerosol Optical Thickness from the GOCART Model and Comparisons with Satellite and Sun Photometer Measurements. Journals of the Atmospheric Sciences, 2002, 59, 461-483.	1.7	1,226
3	Global distribution of UV-absorbing aerosols from Nimbus 7/TOMS data. Journal of Geophysical Research, 1997, 102, 16911-16922.	3.3	995
4	Derivation of aerosol properties from satellite measurements of backscattered ultraviolet radiation: Theoretical basis. Journal of Geophysical Research, 1998, 103, 17099-17110.	3.3	842
5	Aerosols and surface UV products from Ozone Monitoring Instrument observations: An overview. Journal of Geophysical Research, 2007, 112, .	3.3	685
6	Long-term simulation of global dust distribution with the GOCART model: correlation with North Atlantic Oscillation. Environmental Modelling and Software, 2004, 19, 113-128.	4.5	429
7	Validation of the Saharan Dust Plume Conceptual Model Using Lidar, Meteosat, and ECMWF Data. Bulletin of the American Meteorological Society, 1999, 80, 1045-1075.	3.3	322
8	Comparisons of the TOMS aerosol index with Sun-photometer aerosol optical thickness: Results and applications. Journal of Geophysical Research, 1999, 104, 6269-6279.	3.3	272
9	The Ozone Monitoring Instrument: overview of 14 years in space. Atmospheric Chemistry and Physics, 2018, 18, 5699-5745.	4.9	259
10	Tropospheric emissions: Monitoring of pollution (TEMPO). Journal of Quantitative Spectroscopy and Radiative Transfer, 2017, 186, 17-39.	2.3	239
11	Improvements to the OMI near-UV aerosol algorithm using A-train CALIOP and AIRS observations. Atmospheric Measurement Techniques, 2013, 6, 3257-3270.	3.1	187
12	Using the OMI aerosol index and absorption aerosol optical depth to evaluate the NASA MERRA Aerosol Reanalysis. Atmospheric Chemistry and Physics, 2015, 15, 5743-5760.	4.9	184
13	New Era of Air Quality Monitoring from Space: Geostationary Environment Monitoring Spectrometer (GEMS). Bulletin of the American Meteorological Society, 2020, 101, E1-E22.	3.3	165
14	An "A-Train―Strategy for Quantifying Direct Climate Forcing by Anthropogenic Aerosols. Bulletin of the American Meteorological Society, 2005, 86, 1795-1810.	3.3	138
15	Retrieval of Aerosol Optical Depth above Clouds from OMI Observations: Sensitivity Analysis and Case Studies. Journals of the Atmospheric Sciences, 2012, 69, 1037-1053.	1.7	118
16	Earth Observations from DSCOVR EPIC Instrument. Bulletin of the American Meteorological Society, 2018, 99, 1829-1850.	3.3	108
17	Global assessment of OMI aerosol singleâ€scattering albedo using groundâ€based AERONET inversion. Journal of Geophysical Research D: Atmospheres, 2014, 119, 9020-9040.	3.3	102
18	Assessment of OMI nearâ€UV aerosol optical depth over land. Journal of Geophysical Research D: Atmospheres, 2014, 119, 2457-2473.	3.3	101

OMAR TORRES

#	Article	IF	CITATIONS
19	Comparison of Ozone Monitoring Instrument UV Aerosol Products with Aqua/Moderate Resolution Imaging Spectroradiometer and Multiangle Imaging Spectroradiometer observations in 2006. Journal of Geophysical Research, 2008, 113, .	3.3	94
20	Satellite-based evidence of wavelength-dependent aerosol absorption in biomass burning smoke inferred from Ozone Monitoring Instrument. Atmospheric Chemistry and Physics, 2011, 11, 10541-10551.	4.9	94
21	Impacts of brown carbon from biomass burning on surface UV and ozone photochemistry in the Amazon Basin. Scientific Reports, 2016, 6, 36940.	3.3	90
22	Impact of the ozone monitoring instrument row anomaly on the long-term record of aerosol products. Atmospheric Measurement Techniques, 2018, 11, 2701-2715.	3.1	85
23	Passive remote sensing of altitude and optical depth of dust plumes using the oxygen A and B bands: First results from EPIC/DSCOVR at Lagrangeâ€∃ point. Geophysical Research Letters, 2017, 44, 7544-7554.	4.0	69
24	A Color Ratio Method for Simultaneous Retrieval of Aerosol and Cloud Optical Thickness of Above-Cloud Absorbing Aerosols From Passive Sensors: Application to MODIS Measurements. IEEE Transactions on Geoscience and Remote Sensing, 2013, 51, 3862-3870.	6.3	66
25	Stratospheric Injection of Massive Smoke Plume From Canadian Boreal Fires in 2017 as Seen by DSCOVRâ€EPIC, CALIOP, and OMPSâ€LP Observations. Journal of Geophysical Research D: Atmospheres, 2020, 125, e2020JD032579.	3.3	63
26	Comparison of TOMS and AVHRR volcanic ash retrievals from the August 1992 eruption of Mt. Spurr. Geophysical Research Letters, 1999, 26, 455-458.	4.0	57
27	Stratospheric impact of the Chisholm pyrocumulonimbus eruption: 1. Earthâ€viewing satellite perspective. Journal of Geophysical Research, 2008, 113, .	3.3	45
28	OMI tropospheric NO ₂ air mass factors over South America: effects of biomass burning aerosols. Atmospheric Measurement Techniques, 2015, 8, 3831-3849.	3.1	43
29	Detecting layer height of smoke aerosols over vegetated land and water surfaces via oxygen absorption bands: hourly results from EPIC/DSCOVR in deep space. Atmospheric Measurement Techniques, 2019, 12, 3269-3288.	3.1	40
30	Inverse modeling of biomass burning emissions using Total Ozone Mapping Spectrometer aerosol index for 1997. Journal of Geophysical Research, 2005, 110, .	3.3	39
31	Constraining black carbon aerosol over Asia using OMI aerosol absorption optical depth and the adjoint of GEOS-Chem. Atmospheric Chemistry and Physics, 2015, 15, 10281-10308.	4.9	39
32	Direct radiative effect of aerosols based on PARASOL and OMI satellite observations. Journal of Geophysical Research D: Atmospheres, 2017, 122, 2366-2388.	3.3	38
33	Retrieving Aerosol Characteristics From the PACE Mission, Part 2: Multi-Angle and Polarimetry. Frontiers in Environmental Science, 2019, 7, .	3.3	37
34	TROPOMI aerosol products: evaluation and observations of synoptic-scale carbonaceous aerosol plumes during 2018–2020. Atmospheric Measurement Techniques, 2020, 13, 6789-6806.	3.1	36
35	Retrieving Aerosol Characteristics From the PACE Mission, Part 1: Ocean Color Instrument. Frontiers in Earth Science, 2019, 7, .	1.8	31
36	The long-term transport and radiative impacts of the 2017 British Columbia pyrocumulonimbus smoke aerosols in the stratosphere. Atmospheric Chemistry and Physics, 2021, 21, 12069-12090.	4.9	31

OMAR TORRES

#	Article	IF	CITATIONS
37	Insight into global trends in aerosol composition from 2005 to 2015 inferred from the OMI Ultraviolet Aerosol Index. Atmospheric Chemistry and Physics, 2018, 18, 8097-8112.	4.9	30
38	Early calibration problems detected in TOMS Earth-Probe aerosol signal. Geophysical Research Letters, 2007, 34, .	4.0	29
39	Temporal Characterization of Dust Activity in the Central Patagonia Desert (Years 1964–2017). Journal of Geophysical Research D: Atmospheres, 2019, 124, 3417-3434.	3.3	29
40	AEROCOM and AEROSAT AAOD and SSA study – PartÂ1: Evaluation and intercomparison of satellite measurements. Atmospheric Chemistry and Physics, 2021, 21, 6895-6917.	4.9	27
41	Simulation of the transport, vertical distribution, optical properties and radiative impact of smoke aerosols with the ALADIN regional climate model during the ORACLES-2016 and LASIC experiments. Atmospheric Chemistry and Physics, 2019, 19, 4963-4990.	4.9	25
42	A 12-year long global record of optical depth of absorbing aerosols above the clouds derived from the OMI/OMACA algorithm. Atmospheric Measurement Techniques, 2018, 11, 5837-5864.	3.1	21
43	What factors control the trend of increasing AAOD over the United States in the last decade?. Journal of Geophysical Research D: Atmospheres, 2017, 122, 1797-1810.	3.3	20
44	Simulation of the Ozone Monitoring Instrument aerosol index using the NASA Goddard Earth Observing System aerosol reanalysis products. Atmospheric Measurement Techniques, 2017, 10, 4121-4134.	3.1	19
45	Tracking aerosols and SO ₂ clouds from the Raikoke eruption: 3D view from satellite observations. Atmospheric Measurement Techniques, 2021, 14, 7545-7563.	3.1	18
46	Validating MODIS above-cloud aerosol optical depth retrieved from "color ratio―algorithm using direct measurements made by NASA's airborne AATS and 4STAR sensors. Atmospheric Measurement Techniques, 2016, 9, 5053-5062.	3.1	17
47	The role of cloud contamination, aerosol layer height and aerosol model in the assessment of the OMI near-UV retrievals over the ocean. Atmospheric Measurement Techniques, 2016, 9, 3031-3052.	3.1	15
48	Simulation of Optical Properties and Direct and Indirect Radiative Effects of Smoke Aerosols Over Marine Stratocumulus Clouds During Summer 2008 in California With the Regional Climate Model RegCM. Journal of Geophysical Research D: Atmospheres, 2017, 122, 10,312.	3.3	13
49	Retrievals of Aerosol Optical Depth and Spectral Absorption From DSCOVR EPIC. Frontiers in Remote Sensing, 2021, 2, .	3.5	12
50	Explicit Aerosol Correction of OMI Formaldehyde Retrievals. Earth and Space Science, 2019, 6, 2087-2105.	2.6	11
51	Evaluation of the OMPS/LP stratospheric aerosol extinction product using SAGE III/ISS observations. Atmospheric Measurement Techniques, 2020, 13, 3471-3485.	3.1	11
52	Evaluation of Aerosol Properties Observed by DSCOVR/EPIC Instrument From the Earthâ€ S un Lagrange 1 Orbit. Journal of Geophysical Research D: Atmospheres, 2021, 126, e2020JD033651.	3.3	7
53	Hourly Mapping of the Layer Height of Thick Smoke Plumes Over the Western U.S. in 2020 Severe Fire Season. Frontiers in Remote Sensing, 2021, 2, .	3.5	6
54	Detecting Layer Height of Smoke and Dust Aerosols Over Vegetated Land and Water Surfaces via Oxygen Absorption Bands. , 2020, , .		0